HHS Public Access

Author manuscript

J Mol Cell Cardiol. Author manuscript; available in PMC 2020 May 12.

Published in final edited form as:

J Mol Cell Cardiol. 2019 February ; 127: 74–82. doi:10.1016/j.yjmcc.2018.11.014.

Induced *Trf2* deletion leads to aging vascular phenotype in mice associated with arterial telomere uncapping, senescence signaling, and oxidative stress

R. Garrett Morgan[a], **Ashley E. Walker**[a,b], **Daniel W. Trott**[a,b], **Daniel R. Machin**[a,b], **Grant D. Henson**[a,b,c], **Kelly D. Reihl**[a,b], **Richard M. Cawthon**[d], **Eros L. Denchi**[e], **Yu Liu**[a,f], **Samuel I. Bloom**[a], **Tam T. Phuong**[a], **Russell S. Richardson**[a,b,c], **Lisa A. Lesniewski**[a,b], **Anthony J. Donato**[a,b,g,h]

[a]Division of Geriatrics, Department of Internal Medicine, University of Utah School of Medicine, University of Utah, Salt Lake City, Utah, USA

[b]Geriatric Research, Education, and Clinical Center, George E. Wahlen Department of Veterans Affairs Medical Center, Salt Lake City, Utah, USA

[c]Department of Exercise and Sport Science, University of Utah, Salt Lake City, Utah, USA

[d]Department of Human Genetics, University of Utah, Salt Lake City, Utah, USA

[e]Department of Molecular and Experimental Medicine, The Scripps Research Institute, La Jolla, CA, USA

[f]Department of Geriatrics, Tongji Hospital of Tongji Medical College, Huazhong University of Science and Technology, Wuhan, China

[g]Department of Biochemistry, University of Utah, Salt Lake City, Utah, USA

[h]Department of Nutrition and Integrative Physiology, University of Utah, Salt Lake City, Utah, USA

Abstract

Age-related vascular dysfunction in large elastic and resistance arteries is associated with reductions in microvascular perfusion and elevations in blood pressure. Recent evidence indicates that telomere uncapping-induced senescence in vascular cells may be an important source of oxidative stress and vascular dysfunction in aging, but the causal relationship between these processes has yet to be elucidated. To test this important unexplored hypothesis, we measured arterial senescence signaling and oxidative stress, carotid and mesenteric artery endothelium-

Corresponding Author: Please make requests for reprints to: Anthony Donato, Ph.D., Department of Internal Medicine, Division of Geriatrics, University of Utah, Veteran's Affairs Medical Center-SLC, GRECC Building 2, Rm 2D15A, 500 Foothill Drive, Salt Lake City, UT 84148, Tel: (801) 582-1565 Ext 4237, Fax: (801) 585-3884, tony.donato@utah.edu, website: http://www.tvplab.utah.edu.

Disclosure and Conflict of Interest

Dr. Cawthon did not conduct any telomere length measurements for this study, but his patented telomere length measuring technology has been licensed to Telomere Diagnostics, Inc. of Menlo Park, California. No other authors have disclosures or conflicts of interests to report.

dependent vasodilatory capacity, markers of mesenteric microvascular perfusion and endothelial glycocalyx deterioration, and blood pressure in a novel mouse model of Cre-inducible whole body *Trf2* deletion and telomere uncapping. *Trf2* deletion led to a 320% increase in arterial senescence signaling ($P < 0.05$). There was a concurrent 29% and 22% reduction in peak endothelium-dependent vasodilation in carotid and mesenteric arteries, respectively, as well as a 63% reduction in mesenteric microvascular endothelial glycocalyx thickness (all $P \leq 0.01$). Mesenteric microvascular perfusion was reduced by 8% and systolic blood pressure was increased by 9% following *Trf2* deletion (both $P < 0.05$). *Trf2* deletion also led to a pro-oxidative arterial phenotype characterized by increased in NADPH oxidase gene expression; a 210% increase in superoxide levels that was partly dependent on NADPH oxidase activity; and an oxidative stress-mediated reduction in carotid artery vasodilation (all $P \leq 0.05$). Collectively, our findings demonstrate that induced *Trf2* deletion leads to telomere uncapping, increased senescence signaling, and oxidative-stress mediated functional impairments in the vasculature similar to those seen in human aging.

Keywords

vascular aging; telomeres; cellular senescence; oxidative stress

1. Introduction

Advancing age is the primary risk factor for development of vascular functional impairment and cardiovascular disease (CVD)[1]. Endothelial dysfunction in large elastic and resistance arteries is an important age-associated alteration that contributes to reduced microvascular perfusion and elevated blood pressure in older adults[2–5]. Hallmarks of age-related endothelial dysfunction, such as reduced bioavailability of the endothelium-derived vasodilator nitric oxide (NO), impaired endothelium-dependent vasodilation, and degradation of the endothelial glycocalyx (a proteoglycan/glycoprotein layer lining endothelial cells)[6], are due in large part to the accumulation of reactive oxygen species (ROS) like superoxide[7–9]. *In vitro* studies in multiple cell types demonstrate that tumor suppressor protein p53 (p53)-induced senescence leads to increased cellular production and release of ROS generated through increased NADPH oxidase activity[10, 11] and reduced superoxide dismutase activity[12]. Thus, the accumulation of senescent vascular cells with advancing age may be an important mediator of ROS-induced vascular dysfunction. Indeed, our group has recently documented an age-associated upregulation of the p53-induced senescence marker, cyclin-dependent kinase inhibitors 1A (p21), in human endothelial cells and demonstrated its link with endothelial dysfunction[13]. Characterization of the mechanisms that lead to the accumulation of senescent cells in the aging vasculature could prove to be critically important to our understanding of age-associated endothelial dysfunction and CVDs.

Telomere dysfunction is a key age-related process that could lead to cellular senescence, ROS overproduction, and subsequent impairments in vascular function. Telomeres are composed of TTAGGG repeats that form the natural ends of chromosomes and-- along with telomere binding proteins like telomeric repeat binding factor 2 (Trf2)-- generate specialized structures known as t-loops that prevent chromosome ends from being recognized as double-

strand(ds) DNA breaks by the DNA damage repair machinery[14, 15]. Indeed, experimental knockdown of *Trf2* leads to breakdown of the t-loop structure, referred to as telomere uncapping, and initiates a rapid dsDNA break response, p53-mediated upregulation of p21, and cellular senescence[14, 16]. Telomere shortening occurs over time in most tissues, which may lead to critically short telomeres and subsequent uncapping[17, 18]. Alternatively, ROS-mediated damage to telomeric DNA or dysregulation of telomere binding proteins may lead to age-related uncapping without the need for exceptionally short telomeres.

Currently, we have limited observational evidence for the role of telomere uncapping in p53-induced senescence within the human vasculature. These findings suggest that uncapping leads to p53-induced senescence in arteries with advancing age and impaired blood pressure regulation[19, 20]. Despite clear evidence of age-related arterial telomere shortening, age- and hypertension-associated uncapping occurs independent of telomere length[19, 20]. Furthermore, telomere uncapping is correlated with p53-induced senescence while telomere length is not[19, 20]. Importantly, these previous studies demonstrated clear associations between these factors, but did not mechanistically establish telomere uncapping as a cause of age- and hypertension-associated vascular phenotypes. Therefore, an important untested model of human vascular aging predicts that telomere uncapping leads to cellular senescence and elevated ROS in the vasculature, which results in micro- and macro- vascular dysfunction.

In the present study, we hypothesized that *Trf2* deletion results in reduced microvascular perfusion and elevated blood pressure by triggering telomere uncapping, senescence signaling, and ROS-mediated endothelial dysfunction in conduit and resistance arteries. To test this hypothesis, we measured specific markers of arterial p21-induced senescence, carotid and mesenteric artery endothelium-dependent vasodilatory capacity, markers of microvascular perfusion and glycocalyx deterioration, blood pressure, and several key mediators of arterial oxidative stress in a novel mouse model of Cre-inducible whole body *Trf2* deletion mediated telomere uncapping[21].

2. Materials and Methods

2.1. Animals

Conditional whole-body deletion of floxed exons 1 and 2 of the *Trf2* gene was used to induce telomere uncapping in adult mice (aged 4–5 months). Mice that expressed Cre-recombinase in all tissues under control of the tamoxifen-inducible estrogen receptor T2 (CreER) moiety were crossed with mice homozygous for floxed *Trf2* (*Trf2*$^{F/F}$)[21] and wild type *Trf2* (*Trf2*$^{+/+}$) to create compound *Trf2*$^{F/F}$+CreER and *Trf2*$^{+/+}$+CreER mice for use as *Trf2* deficient experimental animals and wild type controls, respectively. *Trf2*$^{+/+}$ mice were derived from the same litters as selected *Trf2*$^{F/F}$ mice to ensure that the final Cre-expressing experimental and wild type control animals had identical compound genetic backgrounds. *Trf2*$^{-/-}$+CreER mice were generated by inducing Cre-recombinase mediated deletion of *Trf2*$^{F/F}$ in all tissues of *Trf2*$^{F/F}$+CreER mice with daily intraperitoneal injections of tamoxifen (1 mg/day) for a total of 4–8 days depending on animal body weight (total tamoxifen given = 200mg-tamoxifen/kg)[22]. Importantly, both *Trf2*$^{F/F}$+CreER mice and

Trf2$^{+/+}$+CreER wild type control mice were injected with identical tamoxifen treatment regimens to control for the effect of tamoxifen in all subsequent analyses (hereafter tamoxifen treated animals are denoted as *Trf2*$^{-/-}$+CreER-POST and *Trf2*$^{+/+}$+CreER-POST mice). Animal breeding and care procedures described in detail in Online Supplement.

2.2. Arterial Trf2 deletion, telomere uncapping, and telomere length

Arterial *Trf2* mRNA expression was determined by qRT-PCR; arterial Trf2 protein by western blot; arterial telomere uncapping by chromatin immunoprecipitation (ChIP); and arterial telomere length by a sequence independent multiplex qPCR technique, as previously described in detail [19] and outlined in Online Supplement.

2.3. Arterial p21-induced senescence signaling markers

p21 protein expression was assessed by fluorescent microscopy in carotid arteries, and arterial *p21* and the ARF variant of cyclin-dependent kinase inhibitor 2A (*p19ARF*) mRNA expression by qRT-PCR, as outlined detail in Online Supplement.

2.4. Carotid and mesenteric artery endothelium-dependent vasodilation: modulation by NO and superoxide

Measurements of endothelial-dependent and endothelial-independent vasodilatory capacity in isolated carotid and mesenteric arteries (2nd order arteries isolated from mesenteric region), and measurements of vasoconstrictor function and myogenic tone in mesenteric arteries, were made using an *ex vivo* method previously described in detail[8] and outlined in Online Supplement.

2.5. Mesenteric microvascular endothelial glycocalyx function and perfusion

Mesenteric microvasculature perfusion, microvessel density, and endothelial glycocalyx function and thickness were measured using a recently validated intravital microscopy technique as previously described in detail[6] and outlined in Online Supplement.

2.6. Blood pressure

2–3 days before and immediately after completing tamoxifen treatment, systolic blood pressure (SBP) was assessed noninvasively in conscious mice by determining the tail blood volume with a volume pressure recording (VPR) sensor and occlusion tail-cuff (CODA System, Kent Scientific) as previously described in detail[8] and outlined in Online Supplement.

2.7. Arterial oxidative stress markers

Arterial NADPH oxidase 1, 2, and 4 (*Nox1*, *Nox2*, and *Nox4)* and superoxide dismutase 1–3 (*Sod1, Sod2,* and *Sod3*) mRNA expression was determined by qRT-PCR, and superoxide content by CMH spin probe and electron paramagnetic resonance spectrometry with and without apocynin and plumbagin mediated Nox activity inhibition, as previously described[8, 23] and outlined in detail in the Online Supplement.

2.8. Statistics

Group mean differences were tested by unpaired and paired sample t-tests with equal variances assumed or multi-factorial ANOVAs with Tukey post-hoc tests. For all dose response and automated capture and analysis measures, group mean differences were tested by two-way repeated-measures ANOVAs with Fisher's LSD post-hoc tests. Alpha was set at $P < 0.05$ and all analyses were completed using GraphPad Prism version 6.0.

3. Results

3.1. Trf2 deletion leads to arterial telomere uncapping with no change in telomere length

Tamoxifen induced Cre-recombinase activation resulted in *loxP* directed deletion of floxed exons 1 and 2 of the *Trf2* gene in arterial tissue from $Trf2^{F/F}$+CreER mice (Figure 1A). *Trf2* deletion resulted in an 85% knockdown of arterial *Trf2* mRNA expression in $Trf2^{-/-}$+CreER-POST mice as compared with $Trf2^{+/+}$+CreER-POST mice ($P = 0.01$; Figure 1B). We confirmed that *Trf2* deletion and knockdown of *Trf2* mRNA expression led to a respective 58% and 42% knockdown of Trf2 protein in a small subset of aortic and mesenteric artery samples from $Trf2^{-/-}$+CreER-POST mice as compared with those from $Trf2^{+/+}$+CreER-POST mice (both $P < 0.01$; Supplemental Figure S1A+B). Accordingly, Trf2 knockdown in $Trf2^{-/-}$+CreER-POST mice led to a 55% increase in arterial telomere uncapping as compared with $Trf2^{+/+}$+CreER-POST mice ($P < 0.05$; Figure 1C). Arterial telomere uncapping in $Trf2^{-/-}$+CreER-POST mice occurred without a change in telomere length ($P = 0.48$; Figure 1D). The level of observed vascular telomere uncapping would roughly correspond to that seen in late middle-aged or early older adult humans (55–60 years of age)[19]. Thus, our whole body *Trf2* deletion system produced an experimental model that was largely representative of the vascular telomere uncapping observed with advancing age in humans.

3.2 Trf2 deletion leads to reductions in body weight and adipose tissue

There was no difference in body weight between $Trf2^{F/F}$+CreER and $Trf2^{+/+}$+CreER mice prior to Cre-recombinase activation ($P = 0.24$). Similarly, there was no body weight difference among $Trf2^{+/+}$+CreER mice before and after Cre activation ($P = 0.48$). A 15% reduction in body weight was observed between $Trf2^{F/F}$+CreER mice and the resulting $Trf2^{-/-}$+CreER-POST mice after Cre activation and *Trf2* deletion ($P < 0.01$), and final body weight was 21% lower in $Trf2^{-/-}$+CreER-POST mice than that of $Trf2^{+/+}$+CreER-POST mice ($P < 0.0001$; Supplemental Table S1). Absolute heart, liver, quadriceps, and epididymal white adipose tissue (WAT) weights in $Trf2^{-/-}$+CreER-POST mice were lower than those of $Trf2^{+/+}$+CreER-POST mice (all $P < 0.02$; Supplemental Table S1). However, when normalized for final body weight, only WAT weight in $Trf2^{-/-}$+CreER-POST mice was lower than that of $Trf2^{+/+}$+CreER-POST mice ($P < 0.01$, Supplemental Table S1).

3.3. Trf2 deletion leads to arterial p21-induced senescence signaling

Trf2 deletion led to a 320% increase in p21 positive cells and 330% increase in *p21* mRNA expression in arterial tissue (both $P \leq 0.03$; Figure 2A+B) in $Trf2^{-/-}$+CreER-POST mice as compared with that from $Trf2^{+/+}$+CreER-POST mice. To rule out the influence of p53

activation and subsequent p21 up-regulation that may have occurred independent of *Trf2* deletion and telomere uncapping, we measured the expression of *p19ARF*, which is a p53 activating protein that is responsive to cellular stress signals in mammalian cells, but not DNA damage response signaling[24]. There was no difference in arterial *p19ARF* mRNA expression between $Trf2^{-/-}$+CreER-POST and $Trf2^{+/+}$+CreER-POST mice ($P = 0.33$; Figure 2C).

3.4 Trf2 deletion leads to impaired endothelium-dependent vasodilatory capacity in carotid and mesenteric arteries

Endothelium-dependent dilation (EDD) in response to the endothelium-specific vasodilator, acetylcholine (ACh), was reduced in isolated carotid and mesenteric arteries from $Trf2^{-/-}$+CreER-POST mice as compared with those from $Trf2^{+/+}$+CreER-POST mice (31% and 22% reduction in max dilation, respectively; both $P < 0.01$; Figure 3A+B).

Incubation with N^G-nitro-L-arginine methyl ester (LNAME), a non-selective endothelial nitric oxide synthase inhibitor, did not further reduce EDD to ACh in carotid or mesenteric arteries from $Trf2^{-/-}$+CreER-POST mice (both $P \geq 0.17$ vs. ACh alone; Figure 3A+B), but reduced that in carotid and mesenteric arteries from $Trf2^{+/+}$+CreER-POST mice (22% and 52% reduction in max dilation vs. ACh alone, respectively; both $P < 0.001$; Figure 3A+B). This abolished the group difference in vasodilatory response to ACh in both artery types (both $P \geq 0.54$), which demonstrates that the EDD impairment observed in $Trf2^{-/-}$+CreER-POST mice was NO-dependent. The reduction in peak EDD to ACh in the presence of LNAME (max dilation to ACh minus max dilation to ACh+LNAME), which represents NO-mediated vasodilation, was 24% lower in carotid arteries and 26% lower in mesenteric arteries from $Trf2^{-/-}$+CreER-POST mice than those from $Trf2^{+/+}$+CreER-POST mice (both $P \leq 0.01$; Figure 3C+D).

There was no difference in carotid or mesenteric artery dilation to the endothelium-independent vasodilator, sodium nitroprusside, between $Trf2^{-/-}$+CreER-POST and $Trf2^{+/+}$+CreER-POST mice (both $P \geq 0.50$; Figure 3E+F), which suggests the group difference in EDD was not due to vascular smooth muscle dysfunction. Furthermore, we found no difference in maximum carotid artery diameter between $Trf2^{-/-}$+CreER-POST and $Trf2^{+/+}$+CreER-POST mice as determined by passive distention response to increasing intraluminal pressure (448.0 ± 16.4 μm vs 448.4 ± 19.9 μm, respectively; $P = 0.49$). There was no group difference in mesenteric artery constriction in response to the α-adrenergic agonist, phenylephrine (PE)(max constriction to PE in $Trf2^{-/-}$+CreER-POST mice: 45.0 ± 8.2% vs. $Trf2^{+/+}$+CreER-POST mice: 43.0 ± 8.3%; $P = 0.79$), which demonstrates that the mesenteric artery EDD impairment observed in $Trf2^{-/-}$+CreER-POST mice was not due to increased sensitivity to adrenergic signaling. To confirm that the selected mesenteric arteries were indeed 2nd order mesenteric arteries capable of generating myogenic tone, we measured spontaneous tone in each group. Mesenteric arteries from $Trf2^{-/-}$+CreER-POST mice had a starting diameter of 163±7 μm and maximum diameter of 206±6 μm, while those from $Trf2^{-/-}$+CreER-POST mice had a starting diameter of 150±6 μm and maximum diameter of 191±5 μm, which represents a respective myogenic tone capacity of 20±3% and 21±2%. Myogenic tone capacity was not different between groups ($P = 0.63$).

3.5. Trf2 deletion leads to impaired mesenteric microvascular perfusion and endothelial glycocalyx deterioration

Microvascular perfusion, assessed by measuring the red blood cell (RBC) fraction across a range of mesenteric microvessel diameters with an automated capture and analysis system, was reduced by 11% in *Trf2*$^{-/-}$+CreER-POST mice as compared with *Trf2*$^{+/+}$+CreER-POST mice ($P = 0.03$; Figure 4A+B), despite no group difference in total mesenteric microvessel density (3841 ± 290 vs. 4298 ± 193 μm/mm^2, respectively; $P = 0.12$). Likewise, *Trf2* deletion led to a 41% reduction in total perfused microvessel density (*Trf2*$^{-/-}$+CreER-POST mice: 1681 ± 139 μm/mm^2 vs. *Trf2*$^{+/+}$+CreER-POST mice: 2871 ± 144; $P < 0.0001$). Mesenteric microvascular endothelial glycocalyx dysfunction was assessed by measuring the depth of RBC penetration into the endothelial glycocalyx (termed perfused boundary region) across a range of mesenteric microvessel diameters utilizing the same automated system. There was a 20% increase in the perfused boundary region of *Trf2*$^{-/-}$+CreER-POST mice as compared with *Trf2*$^{+/+}$+CreER-POST mice ($P = 0.02$; Figure 4C+D), which signifies endothelial glycocalyx deterioration in *Trf2*$^{-/-}$+CreER-POST mice. Accordingly, using a separate manual method to assess glycocalyx thickness, there was a 63% reduction in endothelial glycocalyx thickness in mesenteric microvessels in *Trf2*$^{-/-}$+CreER-POST mice as compared with *Trf2*$^{+/+}$+CreER-POST mice (0.34 ± 0.07 vs. 0.92 ± 0.07 μm, respectively; $P < 0.0001$).

3.6. Trf2 deletion leads to increased blood pressure

SBP increased by approximately 11 mmHg following *Trf2* deletion in *Trf2*$^{F/F}$+CreER mice ($P < 0.05$; Figure 4E), while SBP did not change following Cre-recombinase activation in *Trf2*$^{+/+}$+CreER-POST mice ($P \geq 0.43$; Figure 4E). Heart rate decreased during post-testing in both *Trf2*$^{-/-}$+CreER-POST and *Trf2*$^{+/+}$+CreER-POST mice (both $P < 0.05$; Figure 4F), but there was no group difference in final heart rate ($P = 0.25$; Figure 4F). This indicates that increased heart rate and/or altered autonomic nervous system function were not responsible for the observed changes in blood pressure and group differences in microvascular perfusion.

3.7. Trf2 deletion leads to a pro-oxidative arterial phenotype and ROS-mediated endothelial dysfunction in carotid arteries

We found 28% and 186% increases in *Nox2* and *Nox4* mRNA expression, respectively, in arterial tissue from *Trf2*$^{-/-}$+CreER-POST mice as compared with that from *Trf2*$^{+/+}$+CreER-POST mice (both $P < 0.05$; Figure 5A). Arterial *Nox1* mRNA expression was not different between *Trf2*$^{-/-}$+CreER-POST mice and *Trf2*$^{+/+}$+CreER-POST mice ($P = 0.14$; Figure 5A). Likewise, mRNA expression of the antioxidant enzymes, *Sod1, Sod2,* and *Sod3,* in arterial tissue from *Trf2*$^{-/-}$+CreER-POST mice was not different as compared with that from *Trf2*$^{+/+}$+CreER-POST mice (all $P \geq 0.06$; Figure 5B).

There was also a 210% increase in superoxide levels in arterial tissue from *Trf2*$^{-/-}$+CreER-POST mice as compared with that from *Trf2*$^{+/+}$+CreER-POST mice ($P < 0.01$; Figure 5C). In a small subset of samples, we treated arterial tissue with the non-selective Nox inhibitor, apocynin, and Nox4 inhibitor, plumbagin, prior to assessment of superoxide levels. Superoxide levels remained 2.6 to 4.4 fold higher in arterial tissue from *Trf2*$^{-/-}$+CreER-

POST mice than that from *Trf2*$^{+/+}$+CreER-POST mice following treatment with either apocynin or plumbagin, but were reduced by 65% and 32% in *Trf2*$^{-/-}$+CreER-POST mice, respectively, compared with vehicle treatment (all $P < 0.05$; Supplemental Figure S2). This exploratory result indicates that elevated superoxide content in arteries following *Trf2* deletion was mediated in part by NADPH oxidase activity.

Incubation of carotid arteries with 4-hydroxy-2,2,6,6-tetramethylpiperidin-1-oxyl (TEMPOL), a superoxide scavenger, restored EDD to ACh in *Trf2*$^{-/-}$+CreER-POST as compared with ACh alone in *Trf2*$^{+/+}$+CreER-POST mice ($P = 0.15$; Figure 5D), which demonstrates that the observed reduction in carotid artery EDD in *Trf2*$^{-/-}$+CreER-POST mice was dependent on superoxide activity. Incubation with LNAME in the presence of TEMPOL abolished the selective TEMPOL-mediated restoration of EDD to ACh in *Trf2*$^{-/-}$+CreER-POST mice and EDD response to ACh in *Trf2*$^{+/+}$+CreER-POST mice (both $P \leq 0.01$ vs. ACh+TEMPOL; Figure 5D). There was no group difference following TEMPOL +LNAME treatment ($P = 0.51$; Figure 5D). These results demonstrate that superoxide consumption of NO mediates impaired carotid artery EDD in *Trf2*$^{-/-}$+CreER-POST mice.

4. Discussion

The key novel findings are as follows: First, Cre-induced whole body *Trf2* deletion in mice leads to arterial telomere uncapping and p21-induced senescence signaling without changes in telomere length, thus establishing an experimental system that models arterial telomere uncapping in human aging. Next, we demonstrated that *Trf2* deletion leads to micro- and macro- vascular dysfunction similar to that seen in human aging. The observed dysfunction is characterized by attenuated endothelium-dependent vasodilation in carotid and mesenteric arteries, reduced mesenteric microvascular perfusion and microvascular endothelial glycocalyx deterioration, and increased systolic blood pressure. Last, *Trf2* deletion leads to a pro-oxidative arterial phenotype characterized by increased NADPH oxidase gene expression; increased superoxide levels, mediated in part by NADPH oxidase activity; and superoxide-mediated suppression of carotid artery endothelium-dependent vasodilation. Collectively, our findings demonstrate that experimentally induced *Trf2* deletion in mice leads to oxidative stress mediated functional impairments in the vasculature that phenocopy those seen in human aging.

4.1. Telomere uncapping, p21-induced senescence signaling, and senescence-associated oxidative stress in the vasculature

Telomere uncapping and cellular senescence may be important upstream processes that lead to functional impairments in the vasculature. Prior studies have clearly shown that experimentally induced telomere uncapping leads to p53/p21-induced senescence in multiple cell types and tissues, including vascular cells[14, 16, 21, 25]. The present study, however, is the first to provide evidence that *Trf2* deletion induced *in vivo* leads to telomere uncapping and p21-induced senescence signaling in an otherwise normal vasculature. Here we demonstrate that whole body deletion of *Trf2* results in increased arterial *p21* gene expression and protein upregulation that occurs without a change in telomere length or *p19ARF* expression. p19ARF activates p53 in response to strong mitogenic signals, but not

in response to DNA damage or telomere uncapping[24]. Thus, the observed increase in p21 expression was likely due directly to telomere uncapping and not from any indirect cell signaling effects. These findings provide proof of concept that *Trf2* deletion and resulting telomere uncapping could lead to upregulation of p21-induced senescence markers in arteries, which supports the available observational evidence in humans for a link between arterial telomere uncapping and p53-induced senescence in the context of aging and CVD. Future studies, utilizing p53-null mice or *in vitro* p53 knockdown experiments, are required to conclusively establish a causal relationship between *Trf2* deletion, p53 and vascular functional impairment.

4.2. Trf2 deletion and oxidative stress mediated vascular dysfunction

The release of ROS from senescent cells that accumulate in the vasculature over time could lead to impaired vascular function and contribute to age- and disease-associated phenotypes. In the present study, we demonstrate that *Trf2* deletion leads to higher *Nox2/4* gene expression and increased superoxide levels in arteries concomitant with p21-induced senescence signaling. A set of exploratory experiments that we conducted indicate that the *Trf2* deletion induced increase in superoxide levels is mediated in part by NADPH oxidase activity. The specific goal of this study was to establish a causal relationship between *Trf2* deletion and vascular dysfunction, and not to provide a comprehensive assessment of all pathways that mediate this relationship. However, we believe these findings support our hypothesis that telomere uncapping mediated senescence leads to a pro-oxidative vascular phenotype that is characterized by increased superoxide production mediated in part by increased NADPH oxidase expression.

Evidence from human and animal studies clearly demonstrates that ROS-mediated consumption of NO leads to reduced NO bioavailability and impaired endothelium-dependent vasodilation in aging[8, 9]. Rapid deterioration of the endothelial glycocalyx occurs as a result of ROS accumulation in the vasculature, and can further exacerbate vasodilatory impairments by altering NO release[26, 27]. Here we demonstrate that *Trf2* deletion leads to reduced endothelium-dependent vasodilatory capacity in carotid and mesenteric arteries. These impairments occurred without evidence of vascular smooth muscle or vasoconstrictor dysfunction, as demonstrated by intact vasodilatory responses to an endothelium-independent dilator (SNP) and α-adrenergic agonist (PE). That said, we cannot rule out the potential influence of other aspects of smooth muscle function that may be impaired following *Trf2* deletion and telomere uncapping. We further demonstrate that *Trf2* deletion mediated impairments in vasodilatory capacity are due to reduced NO bioavailability in both artery types and that the reduction in NO bioavailability in carotid arteries was the result of ROS-mediated consumption of NO. We also assessed mesenteric microvascular glycocalyx function using a recently validated automated capture and analysis system that measures the thickness of the glycocalyx layer and the extent of RBC encroachment into the vessel wall due to thinning of the glycocalyx[6]. Utilizing this system we found clear evidence of a diminished endothelial glycocalyx layer similar to that seen in normal vascular aging[6].

Impaired endothelium-dependent vasodilation can lead to increased local vascular tone, which can in turn reduce blood flow to the microvasculature[5] and elevate systolic blood pressure as a consequence of developing less compliant conduit and blood pressure regulating resistance arteries [2–4, 28]. Furthermore, endothelial glycocalyx dysfunction can independently mediate blood pressure dysregulation by disrupting sodium resorption through the microvascular endothelium[27, 29]. Here we found that *Trf2* deletion led to reduced perfusion in the mesenteric microvasculature despite no change in total microvascular density. *Trf2* deletion also led to increased systolic blood pressure, which supports recent observational evidence in humans linking arterial telomere uncapping, p53-induced senescence, and hypertension[20]. Interestingly, heart rate decreased during post-testing in both $Trf2^{-/-}$+CreER-POST and $Trf2^{+/+}$+CreER-POST mice, which may have been the result of tamoxifen induced bradycardia as observed in some human case studies[30, 31]. The observed change in blood pressure, however, was relatively modest and did not lead to clinical hypertension in our experimental animals. Importantly, this effect on blood pressure occurred without the influence of other cardiovascular insults. In the context of normal aging, older adults will accumulate uncapped telomeres within their vascular cells along with a variety of other age-related vascular changes not associated with telomere dysfunction. Collectively, these factors will contribute to the typical magnitude of blood pressure increase seen in normal human aging. Thus, these results may demonstrate the independent influence of telomere uncapping on blood pressure.

4.3 Experimental considerations

While tissue-specific *Trf2* deletion models would demonstrate the functional effects of telomere uncapping in different vascular cell types, age- and disease-associated telomere uncapping may occur in a variety of cellular sources that impact vascular function, including endothelial cells, vascular smooth muscle cells, and immune cells. Thus, we believe the selected model of inducible whole body *Trf2* deletion provides the most accurate representation of *in vivo* telomere uncapping in humans and its downstream effects in the vasculature. Likewise, current evidence for vascular telomere uncapping in humans is limited to data generated from whole artery tissue samples rather than that from specific vascular cell types. Therefore, we focused our experimental outcomes on vascular function endpoints and whole artery assays to better model the design of relevant human tissue studies and provide the most direct test of our stated hypothesis. We believe this experimental system was the most appropriate choice for this initial proof of concept study; however, future studies may utilize tissue-specific *Trf2* deletion models to determine the relative contributions of different vascular cell types to the observed phenotypes.

5. Conclusions

The overall aim of this study was to determine if experimentally induced *Trf2* deletion in mice results in phenotypic changes and functional outcomes in the vasculature similar to those seen in human aging. Our findings demonstrate that *Trf2* deletion leads to arterial telomere uncapping and p21-induced senescence signaling, endothelial dysfunction in carotid and mesenteric arteries, mesenteric microvascular perfusion impairments, and increased systolic blood pressure. These findings also demonstrate that *Trf2* deletion

mediates vascular dysfunction through a pro-oxidative arterial phenotype and ROS-mediated impairments in endothelial function. We believe this study provides the mechanistic foundation for future studies aimed at establishing the prognostic value of telomere uncapping as a biomarker for vascular aging and CVD. Furthermore, these findings have revealed novel pathways involved in telomere uncapping associated vascular dysfunction, which may lead to the identification of pharmacological and/or behavioral interventions that can slow or reverse age-associated vascular dysfunction.

Supplementary Material

Refer to Web version on PubMed Central for supplementary material.

Acknowledgements

R. Garrett Morgan and Anthony J. Donato contributed to all aspects of the study, while remaining authors contributed to the collection and analysis of data, and revision of this manuscript. Eros L. Denchi, Richard M. Cawthon, and Russell S. Richardson further contributed essential reagents and analytical tools.

Funding Sources

Funding: This work was supported by the National Institutes of Health [R01AG040297, R01AG050238, R44AG053131, R21AG033755, and K02AG045339].

References

[1]. Lakatta EG, Arterial and Cardiac Aging: Major Shareholders in Cardiovascular Disease Enterprises: Part I: Aging Arteries: A “Set Up” for Vascular Disease, Circulation 107(1) (2003) 139–146. [PubMed: 12515756]

[2]. Luscher TF, Dohi Y, Tschudi M, Endothelium-dependent regulation of resistance arteries: alterations with aging and hypertension, J Cardiovasc Pharmacol 19 Suppl 5 (1992) S34–42. [PubMed: 1381793]

[3]. Taddei S, Virdis A, Mattei P, Ghiadoni L, Gennari A, Fasolo CB, Sudano I, Salvetti A, Aging and endothelial function in normotensive subjects and patients with essential hypertension, Circulation 91(7) (1995) 1981–7. [PubMed: 7895356]

[4]. Sander M, Chavoshan B, Victor RG, A large blood pressure-raising effect of nitric oxide synthase inhibition in humans, Hypertension 33(4) (1999) 937–42. [PubMed: 10205227]

[5]. Kirby BS, Voyles WF, Simpson CB, Carlson RE, Schrage WG, Dinenno FA, Endothelium-dependent vasodilatation and exercise hyperaemia in ageing humans: impact of acute ascorbic acid administration, J Physiol 587(Pt 9) (2009) 1989–2003. [PubMed: 19307300]

[6]. Machin DR, Bloom SI, Campbell RA, Phuong TTT, Gates PE, Lesniewski LA, Rondina MT, Donato AJ, Advanced age results in a diminished endothelial glycocalyx, Am J Physiol Heart Circ Physiol (2018).

[7]. Rippe C, Lesniewski L, Connell M, LaRocca T, Donato A, Seals D, Short-term calorie restriction reverses vascular endothelial dysfunction in old mice by increasing nitric oxide and reducing oxidative stress, Aging cell 9(3) (2010) 304–12. [PubMed: 20121721]

[8]. Donato AJ, Walker AE, Magerko KA, Bramwell RC, Black AD, Henson GD, Lawson BR, Lesniewski LA, Seals DR, Life-long caloric restriction reduces oxidative stress and preserves nitric oxide bioavailability and function in arteries of old mice, Aging cell 12(5) (2013) 772–83. [PubMed: 23714110]

[9]. Taddei S, Virdis A, Ghiadoni L, Salvetti G, Bernini G, Magagna A, Salvetti A, Age-related reduction of NO availability and oxidative stress in humans, Hypertension 38(2) (2001) 274–9. [PubMed: 11509489]

[10]. Li JM, Fan LM, George VT, Brooks G, Nox2 regulates endothelial cell cycle arrest and apoptosis via p21cip1 and p53, Free Radic Biol Med 43(6) (2007) 976–86. [PubMed: 17697942]

[11]. Salmeen A, Park BO, Meyer T, The NADPH oxidases NOX4 and DUOX2 regulate cell cycle entry via a p53-dependent pathway, Oncogene 29(31) (2010) 4473–84. [PubMed: 20531308]

[12]. Dhar SK, Xu Y, St Clair DK, Nuclear factor kappaB- and specificity protein 1-dependent p53-mediated bi-directional regulation of the human manganese superoxide dismutase gene, J Biol Chem 285(13) (2010) 9835–46. [PubMed: 20061391]

[13]. Rossman MJ, Kaplon RE, Hill SD, McNamara MN, Santos-Parker JR, Pierce GL, Seals DR, Donato AJ, Endothelial cell senescence with aging in healthy humans: prevention by habitual exercise and relation to vascular endothelial function, Am J Physiol Heart Circ Physiol 313(5) (2017) H890–H895. [PubMed: 28971843]

[14]. d'Adda di Fagagna F, Reaper PM, Clay-Farrace L, Fiegler H, Carr P, Von Zglinicki T, Saretzki G, Carter NP, Jackson SP, A DNA damage checkpoint response in telomere-initiated senescence, Nature 426(6963) (2003) 194–8. [PubMed: 14608368]

[15]. Stansel RM, de Lange T, Griffith JD, T-loop assembly in vitro involves binding of TRF2 near the 3' telomeric overhang, Embo J 20(19) (2001) 5532–40. [PubMed: 11574485]

[16]. Cesare AJ, Kaul Z, Cohen SB, Napier CE, Pickett HA, Neumann AA, Reddel RR, Spontaneous occurrence of telomeric DNA damage response in the absence of chromosome fusions, Nat Struct Mol Biol 16(12) (2009) 1244–51. [PubMed: 19935685]

[17]. Daniali L, Benetos A, Susser E, Kark JD, Labat C, Kimura M, Desai K, Granick M, Aviv A, Telomeres shorten at equivalent rates in somatic tissues of adults, Nat Commun 4 (2013) 1597. [PubMed: 23511462]

[18]. Baird DM, Rowson J, Wynford-Thomas D, Kipling D, Extensive allelic variation and ultrashort telomeres in senescent human cells, Nat Genet 33(2) (2003) 203–7. [PubMed: 12539050]

[19]. Morgan RG, Ives SJ, Lesniewski LA, Cawthon RM, Andtbacka RH, Noyes RD, Richardson RS, Donato AJ, Age-related telomere uncapping is associated with cellular senescence and inflammation independent of telomere shortening in human arteries, Am J Physiol Heart Circ Physiol 305(2) (2013) H251–8. [PubMed: 23666675]

[20]. Morgan RG, Ives SJ, Walker AE, Cawthon RM, Andtbacka RH, Noyes D, Lesniewski LA, Richardson RS, Donato AJ, Role of arterial telomere dysfunction in hypertension: relative contributions of telomere shortening and telomere uncapping, J Hypertens 32(6) (2014) 1293–9. [PubMed: 24686009]

[21]. Lazzerini Denchi E, Celli G, de Lange T, Hepatocytes with extensive telomere deprotection and fusion remain viable and regenerate liver mass through endoreduplication, Genes Dev 20(19) (2006) 2648–53. [PubMed: 17015429]

[22]. Ventura A, Kirsch DG, McLaughlin ME, Tuveson DA, Grimm J, Lintault L, Newman J, Reczek EE, Weissleder R, Jacks T, Restoration of p53 function leads to tumour regression in vivo, Nature 445(7128) (2007) 661–5. [PubMed: 17251932]

[23]. Durrant JR, Seals DR, Connell ML, Russell MJ, Lawson BR, Folian BJ, Donato AJ, Lesniewski LA, Voluntary wheel running restores endothelial function in conduit arteries of old mice: direct evidence for reduced oxidative stress, increased superoxide dismutase activity and down-regulation of NADPH oxidase, J Physiol 587(Pt 13) (2009) 3271–85. [PubMed: 19417091]

[24]. Midgley CA, Desterro JM, Saville MK, Howard S, Sparks A, Hay RT, Lane DP, An N-terminal p14ARF peptide blocks Mdm2-dependent ubiquitination in vitro and can activate p53 in vivo, Oncogene 19(19) (2000) 2312–23. [PubMed: 10822382]

[25]. Wang J, Uryga AK, Reinhold J, Figg N, Baker L, Finigan A, Gray K, Kumar S, Clarke M, Bennett M, Vascular Smooth Muscle Cell Senescence Promotes Atherosclerosis and Features of Plaque Vulnerability, Circulation 132(20) (2015) 1909–19. [PubMed: 26416809]

[26]. Kumagai R, Lu X, Kassab GS, Role of glycocalyx in flow-induced production of nitric oxide and reactive oxygen species, Free Radic Biol Med 47(5) (2009) 600–7. [PubMed: 19500664]

[27]. Reitsma S, Slaaf DW, Vink H, van Zandvoort MA, oude Egbrink MG, The endothelial glycocalyx: composition, functions, and visualization, Pflugers Arch 454(3) (2007) 345–59. [PubMed: 17256154]

[28]. Fujii K, Tominaga M, Ohmori S, Kobayashi K, Koga T, Takata Y, Fujishima M, Decreased endothelium-dependent hyperpolarization to acetylcholine in smooth muscle of the mesenteric artery of spontaneously hypertensive rats, Circ Res 70(4) (1992) 660–9. [PubMed: 1551193]

[29]. Oberleithner H, Two barriers for sodium in vascular endothelium?, Ann Med 44 Suppl 1 (2012) S143–8. [PubMed: 22471931]

[30]. Slovacek L, Priester P, Petera J, Slanska I, Kopecky J, Tamoxifen/norfloxacin interaction leading to QT interval prolongation in a female patient with extracranial meningioma, Bratisl Lek Listy 112(6) (2011) 353–4. [PubMed: 21692412]

[31]. Slovacek L, Ansorgova V, Macingova Z, Haman L, Petera J, Tamoxifen-induced QT interval prolongation, J Clin Pharm Ther 33(4) (2008) 453–5. [PubMed: 18613864]

10.

Highlights

1. Evidence of causal link between telomere uncapping and vascular dysfunction.
2. Supports observational link between arterial telomere uncapping and hypertension
3. Demonstrate that *Trf2* deletion leads to ROS-mediated endothelial dysfunction.

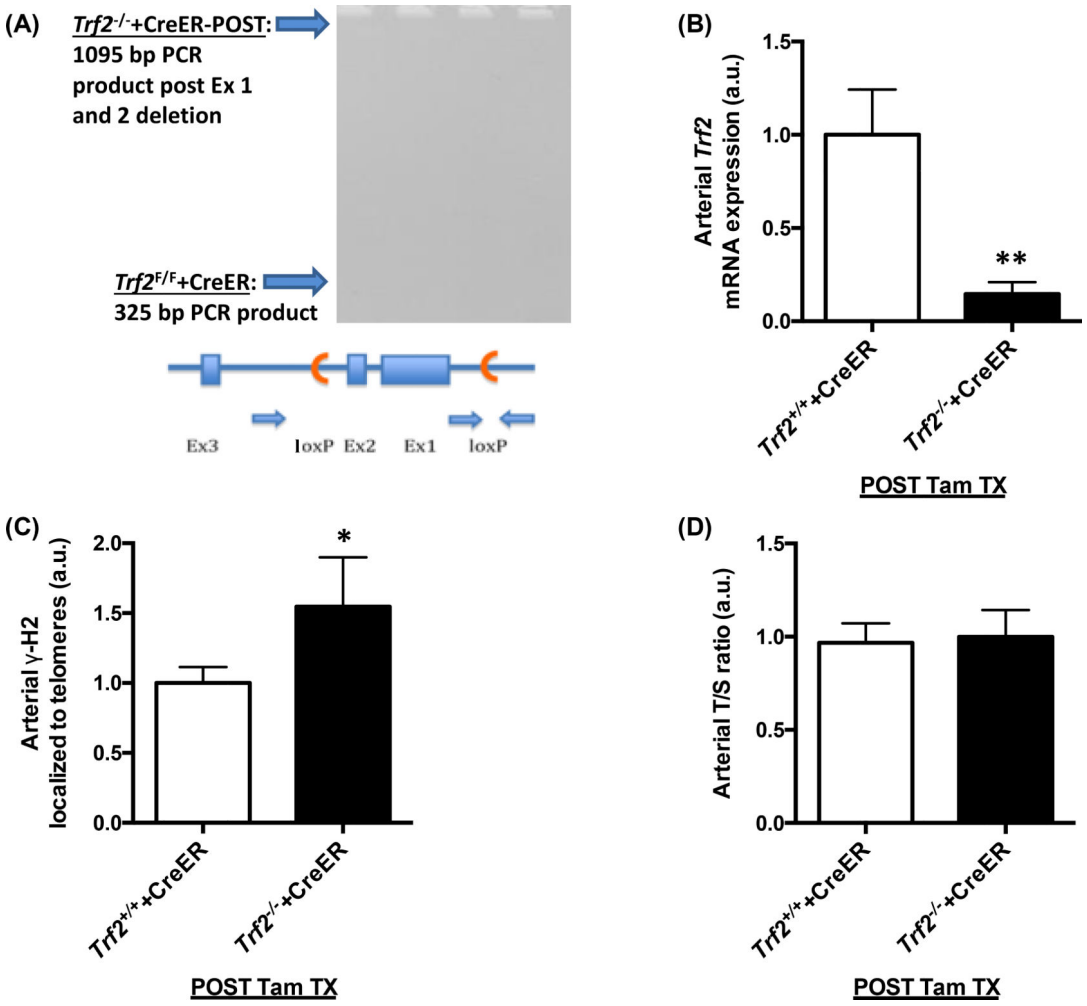

Figure 1. *Trf2* gene deletion and arterial telomere uncapping.

Representative DNA gel images with genotypespecific PCR products (cropped to shape) and diagram demonstrating *loxP* directed deletion of exons 1 and 2 from *Trf2* gene in arterial tissue from $Trf2^{F/F}$+CreER mice (A). Arterial *Trf2* mRNA expression (B), telomere uncapping (C), and telomere length (D) in $Trf2^{+/+}$+CreER-POST and $Trf2^{-/-}$+CreER-POST mice (n = 6–11 per group). mRNA is expressed relative to 18s rRNA expression to account for differences in total RNA. ChIP data is expressed relative to input telomeric DNA content to account for differences in cell number. Data presented are means ± SEM normalized to $Trf2^{+/+}$+CreER-POST mean. *$P < 0.05$ and **$P = 0.01$ vs. $Trf2^{+/+}$+CreER-POST mice. Terms: Trf2, telomeric repeat binding factor 2; CreER, Cre-recombinase associated with estrogen receptor T2; POST/POST Tam TX, post tamoxifen treatment; ex, exon; bp, base pair; F/F, homozygous floxed allele; γ-H2, p-histone γ-H2A.X (ser139); and T/S, telomeric DNA/single copy gene signals.

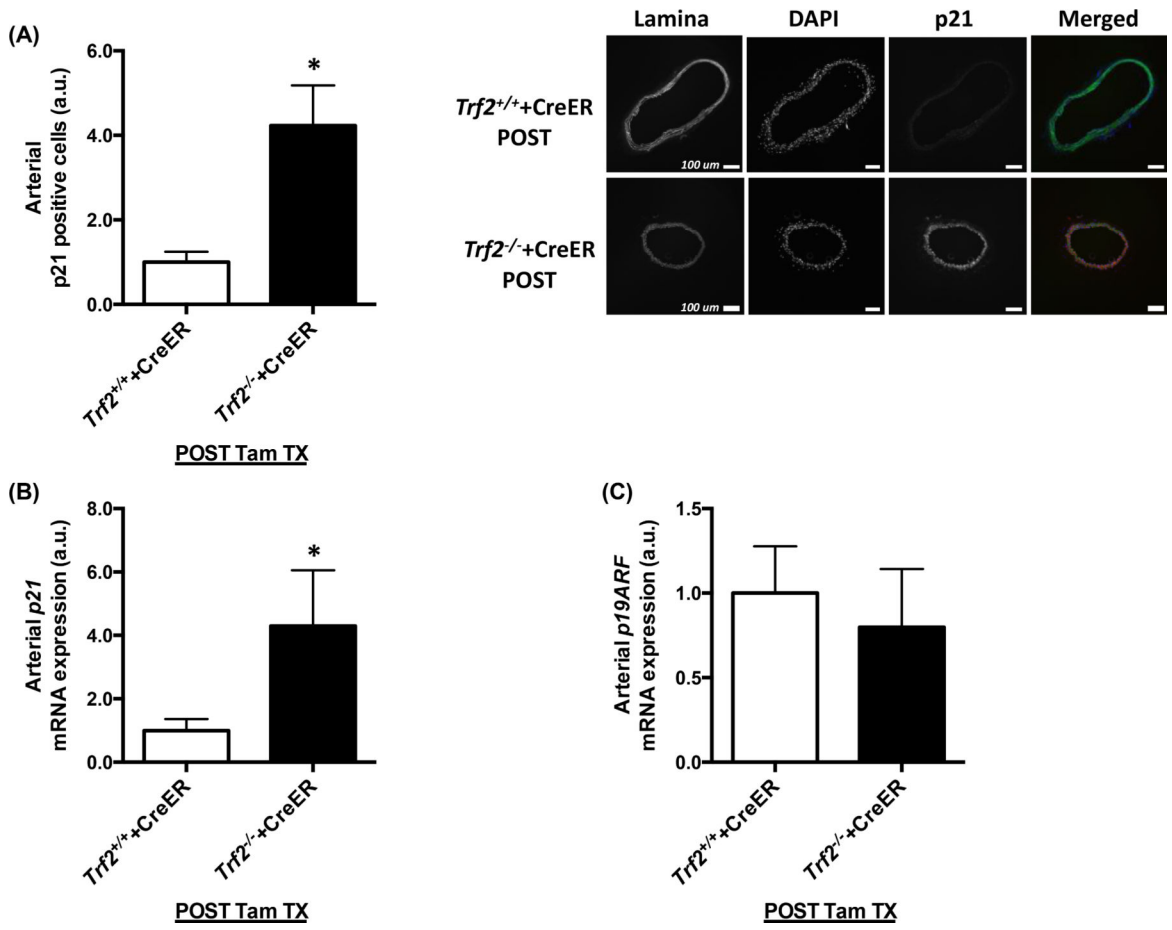

Figure 2. *Trf2* deletion and arterial p21-induced senescence signaling.

Arterial p21 positive cells (A), *p21* mRNA expression (B), and *p19ARF* mRNA expression (C) in $Trf2^{+/+}$+CreER-POST and $Trf2^{-/-}$+CreER-POST mice (n = 3–8 per group). mRNA is expressed relative to 18s rRNA expression to account for differences in total RNA. p21 positive cells are expressed relative to DAPI nuclear staining signal to account for differences in cell number. Representative images of carotid artery lamina auto-fluorescence (FITC channel), DAPI staining (DAPI channel), p21 protein staining (Cy5 channel), and merged image shown next to panel (A) (images cropped to shape; scale bars = 100 μm). Relative size of arteries shown is not representative of mean difference in carotid artery diameter between groups (see Results section 3.4). Data presented are means ± SEM normalized to $Trf2^{+/+}$+CreER-POST mean. $*P < 0.05$ vs. $Trf2^{+/+}$+CreER-POST mice. Terms: p21, cyclin-dependent kinase inhibitor 1A (p21); p19ARF, cyclin-dependent kinase inhibitor 2A (ARF variant); Trf2, telomeric repeat binding factor 2; CreER, Cre-recombinase associated with estrogen receptor T2; POST/POST Tam TX, post tamoxifen treatment; and DAPI, 4’,6-diamidino-2-phenylindole.

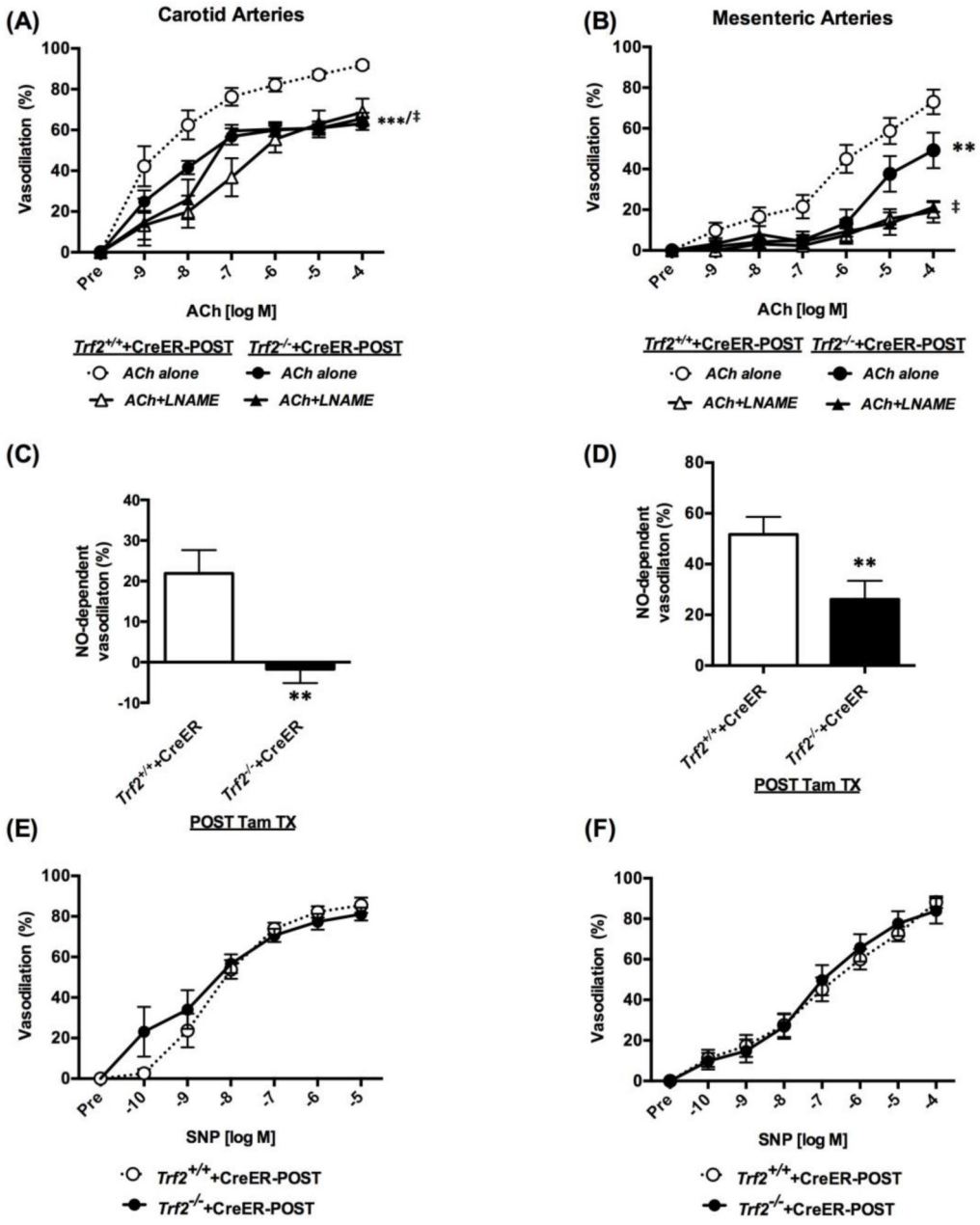

Figure 3. *Trf2* deletion and arterial endothelium-dependent vasodilation.

Vasodilation to ACh alone and in the presence of NO synthase inhibitor, LNAME, in carotid (A) and mesenteric arteries (B), NO-dependent vasodilation in carotid (C) and mesenteric arteries (D), and vasodilation to SNP in carotid (E) and mesenteric arteries (F) from $Trf2^{+/+}$ +CreER-POST and $Trf2^{-/-}$+CreER-POST mice (n = 7–13 per group). Data presented are means ± SEM. $^{**}P \leq 0.01$ and $^{***}P < 0.001$ vs. $Trf2^{+/+}$+CreER-POST mice; and $^{‡}P < 0.05$ vs. ACh alone within group. Terms: Trf2, telomeric repeat binding factor 2; CreER, Cre-recombinase associated with estrogen receptor T2; POST/POST Tam TX, post tamoxifen treatment; ACh, acetylcholine; NO, nitric oxide; LNAME, N^G-nitro-L-arginine methyl ester; and SNP, sodium nitroprusside.

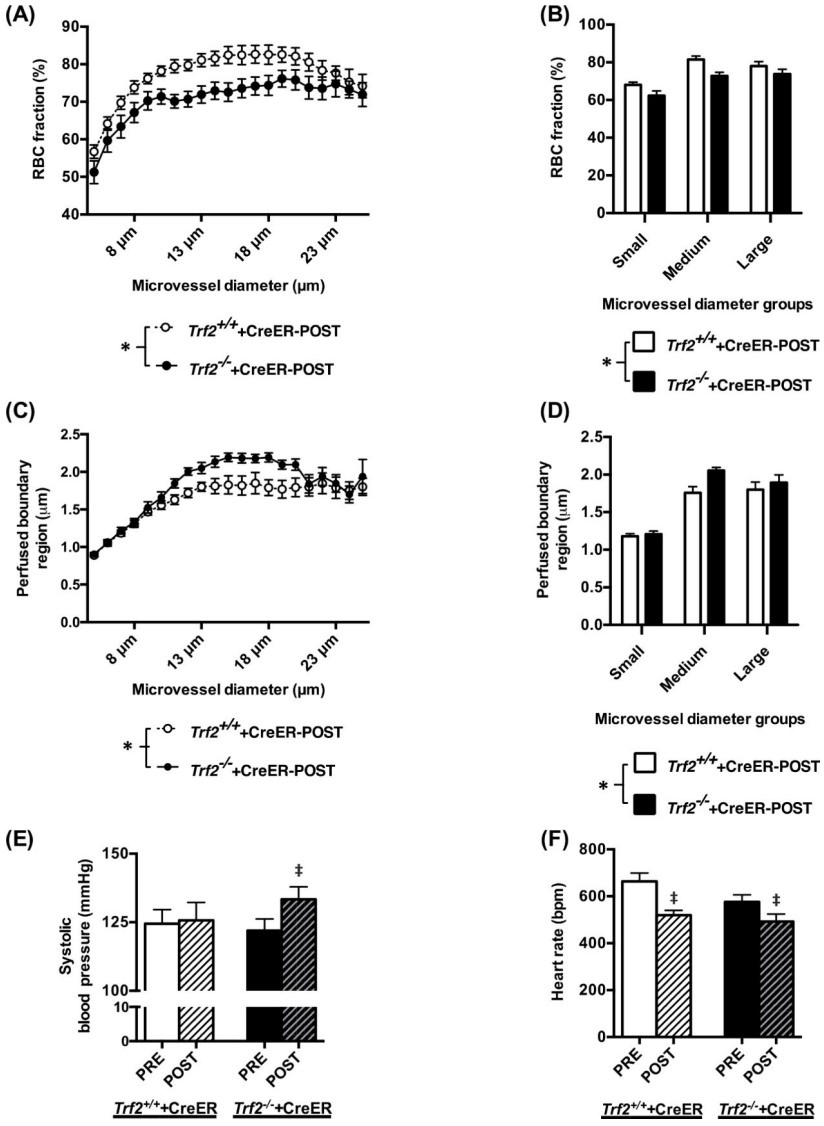

Figure 4. *Trf2* deletion and *in vivo* vascular function.

RBC fraction across the range of measured mesenteric microvessel diameters (A), RBC fraction grouped by small (5–9 μm), medium (10–19 μm), and large (20–25 μm) microvessel diameters (B), perfused barrier region across range of mesenteric microvessel diameters (C), and perfused barrier region grouped by small (5–9 μm), medium (10–19 μm), and large (20–25 μm) microvessel diameters (D) in $Trf2^{+/+}$+CreER-POST and $Trf2^{-/-}$+CreER-POST mice (n = 11–16 per group). Systolic blood pressure (E) and heart rate (F) in $Trf2^{+/+}$+CreER-POST and $Trf2^{-/-}$+CreER-POST mice, before and after Cre-recombinase activation (n = 7 per group). Data presented are means ± SEM. $*P < 0.05$ vs. $Trf2^{+/+}$+CreER-POST mice; and $‡P < 0.05$ following Cre-recombinase activation. The RBC fraction and perfused barrier region within each diameter group (B+D) were not different (all $P \geq 0.07$). Terms: Trf2, telomeric repeat binding factor 2; CreER, Cre-recombinase associated with estrogen receptor T2; POST, post tamoxifen treatment; RBC, red blood cell; Pre, before Cre-recombinase activation; and Post, after Cre-recombinase activation.

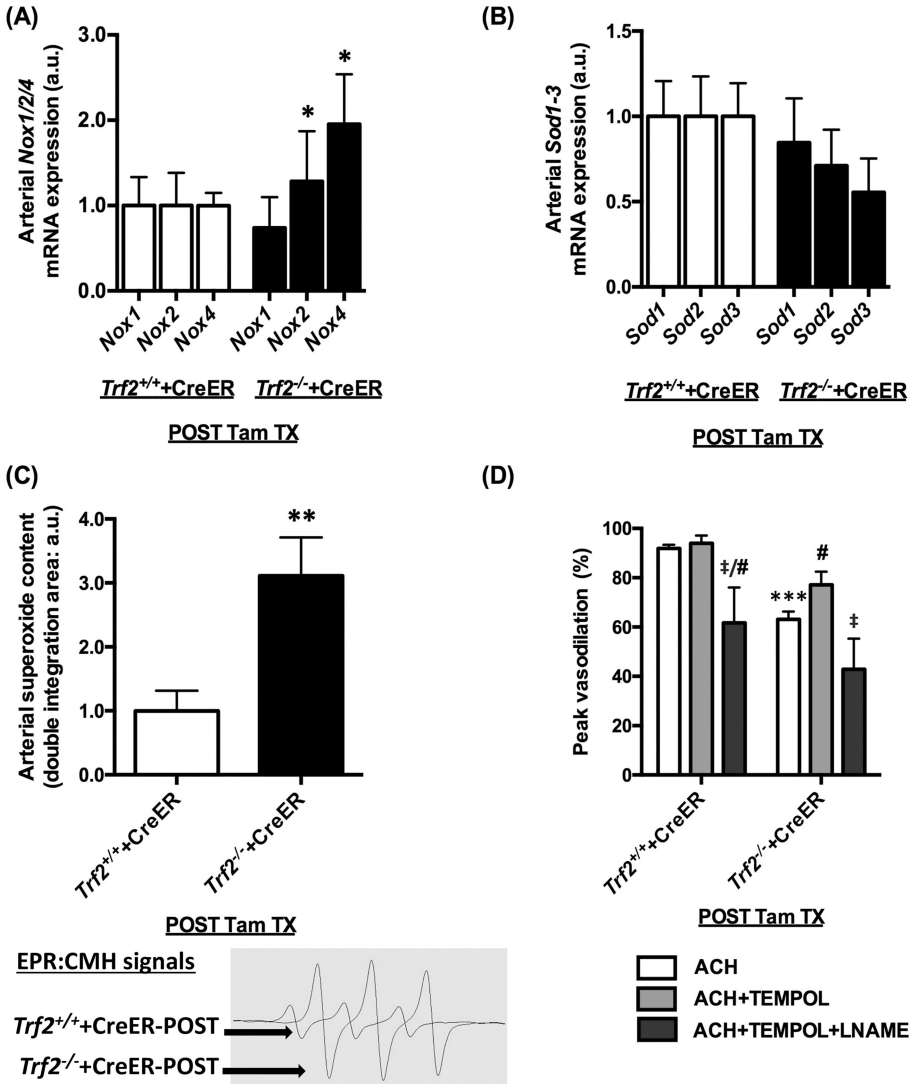

Figure 5. *Trf2* deletion, pro-oxidative arterial phenotype, and ROS-mediated arterial endothelial dysfunction.

Arterial *Nox1*, *Nox2*, and *Nox4* mRNA expression (A); *Sod1*, *Sod2*, and *Sod3* mRNA expression (B); superoxide content (C); and vasodilatory response of carotid arteries to max dose of ACh alone and after pretreatment with NO synthase inhibitor LNAME in the absence or presence of superoxide scavenger TEMPOL (D) in $Trf2^{+/+}$+CreER-POST and $Trf2^{-/-}$+CreER-POST mice (n = 4–15 per group). mRNA is expressed relative to 18s rRNA expression to account for differences in total RNA, and mRNA expression and superoxide content presented normalized to $Trf2^{+/+}$+CreER-POST mean. Representative EPR generated CMH signal curves used to calculate superoxide content shown below panel and cropped to shape(C). Data presented are means ± SEM. $^{*}P < 0.05$, $^{**}P < 0.01$, and $^{***}P < 0.001$ vs. $Trf2^{+/+}$+CreER-POST mice; $^{\#}P < 0.05$ vs. ACh alone within group; and $^{\ddagger}P < 0.05$ vs. ACh +TEMPOL within group. Terms: ROS, reactive oxygen species; Trf2, telomeric repeat binding factor 2; CreER, Cre-recombinase associated with estrogen receptor T2; POST/POST Tam TX, post tamoxifen treatment; Nox, NADPH oxidase; Sod, superoxide dismutase; NO, nitric oxide; EPR, electron paramagnetic resonance; and CMH, 1-

hydroxy-3-methoxycarbonyl-2,2,5,5-tetramethylpyrrolidine; ACh, acetylcholine; LNAME, N^G-nitro-L-arginine methyl ester; and TEMPOL, 4-hydroxy-2,2,6,6-tetramethylpiperidin-1-oxyl.